Journal of Zhejiang University-SCIENCE A (Applied Physics & Engineering)
ISSN 1673-565X (Print); ISSN 1862-1775 (Online)
www.zju.edu.cn/jzus; www.springerlink.com
E-mail: jzus@zju.edu.cn

Control-oriented dynamic identification modeling of a planar SOFC stack based on genetic algorithm-least squares support vector regression*

Hai-bo HUO†1, Yi JI[1], Xin-jian ZHU[2], Xing-hong KUANG[1], Yu-qing LIU[1]

([1]*Department of Electrical Engineering, Shanghai Ocean University, Shanghai 201306, China*)

([2]*Fuel Cell Research Institute, Shanghai Jiao Tong University, Shanghai 200240, China*)

†E-mail: hbhuo@shou.edu.cn

Received Jan. 6, 2014; Revision accepted May 7, 2014; Crosschecked Sept. 29, 2014

Abstract: For predicting the voltage and temperature dynamics synchronously and designing a controller, a control-oriented dynamic modeling study of the solid oxide fuel cell (SOFC) derived from physical conservation laws is reported, which considers both the electrochemical and thermal aspects of the SOFC. Here, the least squares support vector regression (LSSVR) is employed to model the nonlinear dynamic characteristics of the SOFC. In addition, a genetic algorithm (GA), through comparing a simulated annealing algorithm (SAA) with a 5-fold cross-validation (5FCV) method, is preferably chosen to optimize the LSSVR's parameters. The validity of the proposed LSSVR with GA (GA-LSSVR) model is verified by comparing the results with those obtained from the physical model. Simulation studies further indicate that the GA-LSSVR model has a higher modeling accuracy than the LSSVR with SAA (SAA-LSSVR) and the LSSVR with 5FCV (5FCV-LSSVR) models in predicting the voltage and temperature transient behaviors of the SOFC. Furthermore, the convergence speed of the GA-LSSVR model is relatively fast. The availability of this GA-LSSVR identification model can aid in evaluating the dynamic performance of the SOFC under different conditions and can be used for designing valid multivariable control schemes.

Key words: Solid oxide fuel cell (SOFC), Control-oriented, Dynamic modeling, Least squares support vector regression (LSSVR)

doi:10.1631/jzus.A1400011 **Document code:** A **CLC number:** TM911.4

1 Introduction

A solid oxide fuel cell (SOFC) converts gaseous or gasified fuel chemical energy directly into electricity and heat at high temperatures (800–1000 °C). Among various types of fuel cells, SOFC is well known for its high energy conversion efficiency, fuel adaptability, high temperature exhaust gas, and solid state design. In addition, as a promising electricity generation technology, SOFC is particularly attractive for distributed or stationary power plants and mobile applications.

The development of effective control systems is in great demand before achieving successful commercialization of the SOFC. A good dynamic model is becoming a critical tool to study the dynamics of the SOFC, and to design and optimize the stack. Moreover, it is crucial for designing model-based control strategies. In recent years, abundant dynamic models of the SOFC have been developed and researched (Li *et al.*, 2008; Kim *et al.*, 2011; Menon *et al.*, 2012; Jiang *et al.*, 2013; So-ryeok *et al.*, 2013). Whereas, most of these models are unsuitable for model-based control design because they are too complex.

* Project supported by the Ocean Energy Program of State Oceanic Administration (No. SHME2013JS01), and the Shanghai Municipal Natural Science Foundation (No. 12ZR1413100), China

For control applications, a lot of first-principles models represented by first-order ordinary differential equations have been proposed (Salogni and Colonna, 2010; Kazempoor *et al.*, 2011; Hajimolana *et al.*, 2013). However, the solution to these differential equations is very difficult and time-consuming (Wang *et al.*, 2008). By far, several identification models of the SOFC have been reported for predicting performance and control-oriented applications (Jurado, 2004; Huo *et al.*, 2008; Yang *et al.*, 2009; Zhang and Feng, 2009; Wu *et al.*, 2011), which avoids using complicated differential equations to describe the stack. The SOFC dynamic identification models developed by Yang *et al.* (2009) and Wu *et al.* (2011) include temperature and heat transfer dynamics but no electrochemical dynamics. Jurado (2004), Huo *et al.* (2008), and Zhang and Feng (2009) considered the electrochemical characteristics in their identification models. However, it is assumed that the SOFC operating temperature is constant in (Jurado, 2004; Huo *et al.*, 2008; Zhang and Feng, 2009). It is well known that electrochemical reactions are tightly coupled with mass transport, charge transport, and heat transfer (Bove and Ubertini, 2006; Entchev and Yang, 2007). Thus, in the present work, a control relevant dynamic identification model based on the least squares support vector regression with genetic algorithm (GA-LSSVR) by considering both electrochemical and thermal aspects of the SOFC will be presented.

Support vector regression (SVR) is a novel machine-learning method, which is developed based on the principle of structural risk minimization (SRM) from statistical learning theory (SLT). SVR can minimize both evaluated errors and model complexity at the same time, which makes it possess good generalization ability and prevents over-fitting (Qu and Zuo, 2012). Lately, the least squares support vector regression (LSSVR) has grown as a new version of SVR (Suykens *et al.*, 2002). Because it has better generalization capability and can accomplish a global optimal value in a shorter training time, LSSVR has been successfully applied to models in numerous fields (Ge and Song, 2008; Wang *et al.*, 2011; Xu and Huang, 2011).

However, to establish a more accurate LSSVR model, how to select the best hyper-parameters becomes a key problem. Generally, the cross-validation (CV) technique is widely used for optimizing the hyper-parameters of the regression model. Though the CV methods are simplicity, reliability, etc., their computational cost is high (Mao *et al.*, 2011). For building a more accurate LSSVR model for the SOFC, genetic algorithm (GA) is chosen to search the optimal hyper-parameters of the LSSVR in this study.

2 Dynamic physical model of the SOFC

A dynamic physical model of the planar SOFC fed with hydrogen and air mainly considers two dynamic responses: the electrochemical dynamics and the thermal dynamics. The main assumptions of the physical model are as follows (Padullés *et al.*, 2000; Murshed *et al.*, 2007):

(1) All the gases are considered as ideal gases;

(2) The internal operating pressure is constant;

(3) Both anode and cathode channel exhaust gases pass through a single "choked" orifice;

(4) Temperature in the SOFC stack is uniform;

(5) The fuel and air temperatures at the exit of both channels are equal to the inside temperatures;

(6) Heat exchange between the stack and the ambient environment is not taken into account.

2.1 Electrochemical sub-model

The SOFC basic reaction principle is depicted in Fig. 1 (Cao *et al.*, 2010), where TBP is the triple phase boundary. When hydrogen is used as fuel, the SOFC electrochemical reactions are given by

$$\text{Anode:}\quad \mathrm{H_2+O^{2-}\rightarrow H_2O+2e^-}, \tag{1}$$

$$\text{Cathode:}\quad \mathrm{O_2+4e^-\rightarrow 2O^{2-}}, \tag{2}$$

$$\text{Overall reaction:}\quad \mathrm{H_2+\frac{1}{2}O_2\rightarrow H_2O}. \tag{3}$$

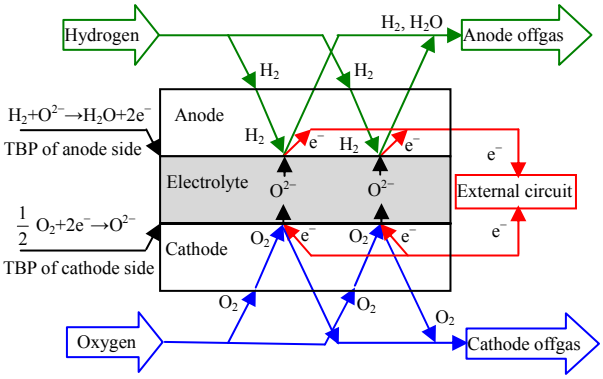

Fig. 1 Basic operating principle of the SOFC

The SOFC electrochemical dynamics can be represented by the concentration changes of the chemical species, which take part in the cell reaction. For ideal gases, the changes of concentration and partial pressure are identical in a vessel with fixed volume (Lu *et al.*, 2006).

2.1.1 Calculation of the partial pressures

Applying the perfect gas equation for hydrogen, we have

$$p_{\mathrm{H}_2} V_{\mathrm{an}} = n_{\mathrm{H}_2} R T_{\mathrm{s}}. \tag{4}$$

Taking the time derivative of the above expression, we can obtain:

$$\frac{\mathrm{d}}{\mathrm{d}t} p_{\mathrm{H}_2} = \frac{R T_{\mathrm{s}}}{V_{\mathrm{an}}} \frac{\mathrm{d}}{\mathrm{d}t} n_{\mathrm{H}_2}. \tag{5}$$

Defining

$$q_{\mathrm{H}_2} = \frac{\mathrm{d}}{\mathrm{d}t} n_{\mathrm{H}_2}, \tag{6}$$

we have

$$\frac{\mathrm{d}}{\mathrm{d}t} p_{\mathrm{H}_2} = \frac{R T_{\mathrm{s}}}{V_{\mathrm{an}}} q_{\mathrm{H}_2}, \tag{7}$$

where p_{H_2}, V_{an}, n_{H_2}, and T_{s} are the partial pressure of hydrogen, the anode compartment volume, the mole number of hydrogen in anode, and the stack temperature, respectively.

The hydrogen molar flow rate q_{H_2} consists of three components: the input flow rate $q_{\mathrm{H}_2}^{\mathrm{in}}$, the reactive flow rate $q_{\mathrm{H}_2}^{\mathrm{r}}$, and the output flow rate $q_{\mathrm{H}_2}^{\mathrm{out}}$. Thus, we can obtain

$$\frac{\mathrm{d}}{\mathrm{d}t} p_{\mathrm{H}_2} = \frac{R T_{\mathrm{s}}}{V_{\mathrm{an}}} (q_{\mathrm{H}_2}^{\mathrm{in}} - q_{\mathrm{H}_2}^{\mathrm{out}} - q_{\mathrm{H}_2}^{\mathrm{r}}). \tag{8}$$

Similarly, the partial pressure of the product water vapor inside the anode channel can be expressed as

$$\frac{\mathrm{d}}{\mathrm{d}t} p_{\mathrm{H_2O}} = \frac{R T_{\mathrm{s}}}{V_{\mathrm{an}}} (0 - q_{\mathrm{H_2O}}^{\mathrm{out}} + q_{\mathrm{H_2O}}^{\mathrm{r}}). \tag{9}$$

Inside the cathode channel, the oxygen partial pressure can be calculated as

$$\frac{\mathrm{d}}{\mathrm{d}t} p_{\mathrm{O}_2} = \frac{R T_{\mathrm{s}}}{V_{\mathrm{ca}}} (q_{\mathrm{O}_2}^{\mathrm{in}} - q_{\mathrm{O}_2}^{\mathrm{out}} - q_{\mathrm{O}_2}^{\mathrm{r}}), \tag{10}$$

where V_{ca} is the cathode compartment volume. From electrochemical properties, we know that (Chakraborty, 2011)

$$q_{\mathrm{H}_2}^{\mathrm{r}} = \frac{I}{2F}. \tag{11}$$

Similarly,

$$q_{\mathrm{H_2O}}^{\mathrm{r}} = \frac{I}{2F}, \tag{12}$$

and

$$q_{\mathrm{O}_2}^{\mathrm{r}} = \frac{I}{4F}, \tag{13}$$

where I is the stack current, and F is Faraday's constant. Defining a constant as follows:

$$K_{\mathrm{r}} = \frac{1}{4F}, \tag{14}$$

we have

$$q_{\mathrm{H}_2}^{\mathrm{r}} = q_{\mathrm{H_2O}}^{\mathrm{r}} = 2K_{\mathrm{r}} I, \tag{15}$$

and

$$q_{\mathrm{O}_2}^{\mathrm{r}} = K_{\mathrm{r}} I. \tag{16}$$

The relation of gas molar flow through the valve and its partial pressure inside the channel can be given as (Padullés *et al.*, 2000)

$$\frac{q_{\mathrm{H}_2}^{\mathrm{out}}}{p_{\mathrm{H}_2}} = K_{\mathrm{H}_2}, \tag{17}$$

$$\frac{q_{\mathrm{H_2O}}^{\mathrm{out}}}{p_{\mathrm{H_2O}}} = K_{\mathrm{H_2O}}, \tag{18}$$

and

$$\frac{q_{\mathrm{O}_2}^{\mathrm{out}}}{p_{\mathrm{O}_2}} = K_{\mathrm{O}_2}. \tag{19}$$

By substituting the expressions of the reaction flow rates and the output flow rates into Eqs. (8)–(10) and applying the Laplace transforms, the dynamic relationships of partial pressure for hydrogen, water, and oxygen can be expressed in the following forms:

$$p_{\mathrm{H}_2} = \frac{1/K_{\mathrm{H}_2}}{1 + \tau_{\mathrm{H}_2} s} (q_{\mathrm{H}_2}^{\mathrm{in}} - 2K_{\mathrm{r}} I), \tag{20}$$

$$p_{\mathrm{H_2O}}=\frac{1/K_{\mathrm{H_2O}}}{1+\tau_{\mathrm{H_2O}}s}2K_{\mathrm{r}}I, \tag{21}$$

$$p_{\mathrm{O_2}}=\frac{1/K_{\mathrm{O_2}}}{1+\tau_{\mathrm{O_2}}s}(q_{\mathrm{O_2}}^{\mathrm{in}}-K_{\mathrm{r}}I), \tag{22}$$

where

$$\tau_{\mathrm{H_2}}=\frac{V_{\mathrm{an}}}{K_{\mathrm{H_2}}RT_{\mathrm{s}}}, \tag{23}$$

$$\tau_{\mathrm{H_2O}}=\frac{V_{\mathrm{an}}}{K_{\mathrm{H_2O}}RT_{\mathrm{s}}}, \tag{24}$$

$$\tau_{\mathrm{O_2}}=\frac{V_{\mathrm{ca}}}{K_{\mathrm{O_2}}RT_{\mathrm{s}}}, \tag{25}$$

where $K_{\mathrm{H_2}}$, $K_{\mathrm{O_2}}$, and $K_{\mathrm{H_2O}}$ are the valve molar constants for hydrogen, oxygen, and water, respectively; $\tau_{\mathrm{H_2}}$, $\tau_{\mathrm{O_2}}$, and $\tau_{\mathrm{H_2O}}$ are the response times for hydrogen flow, oxygen flow, and water flow, respectively; and s is the Laplace operator.

2.1.2 Output voltage of the SOFC

When only ohmic loss is considered, applying Nernst's equation and Ohm's law, the DC output voltage of the SOFC stack consisting of N_0 cells in series is represented by

$$V_{\mathrm{s}}=E-rI, \tag{26}$$

and the open circuit voltage E is

$$E=N_0E_0+\frac{N_0RT_{\mathrm{s}}}{2F}\ln\frac{p_{\mathrm{H_2}}p_{\mathrm{O_2}}^{0.5}}{p_{\mathrm{H_2O}}}, \tag{27}$$

where E_0, N_0, and r are the standard reversible cell potential, the cell numbers in the stack, and the ohmic resistance, respectively.

2.2 Energy balance sub-model

Suppose the SOFC stack is an adiabatic operation. Therefore, the energy consumption into the environment is not considered. It is assumed that the electrode, interconnector, and gases inside the channels of the SOFC are isothermal in any case. Ignoring the gas heat capacities, the energy balance of the SOFC stack can be expressed as (Murshed *et al.*, 2007)

$$\begin{aligned}m_{\mathrm{s}}\bar{c}_{\mathrm{ps}}\frac{\mathrm{d}T_{\mathrm{s}}}{\mathrm{d}t}&=\sum q_i^{\mathrm{in}}\int_{T_{\mathrm{ref}}}^{T_{\mathrm{in}}}c_{\mathrm{p},i}(T)\mathrm{d}T\\&\quad-\sum q_i^{\mathrm{out}}\int_{T_{\mathrm{ref}}}^{T_{\mathrm{s}}}c_{\mathrm{p},i}(T)\mathrm{d}T-q_{\mathrm{H_2}}^{\mathrm{r}}\Delta\hat{H}_{\mathrm{r}}^0-V_{\mathrm{s}}I,\end{aligned} \tag{28}$$

where m_{s} and $\bar{c}_{\mathrm{ps}}$ are the mass and average specific heat of the fuel cell solid materials; $c_{\mathrm{p},i}$ and $\Delta\hat{H}_{\mathrm{r}}^0$ are the specific heat of species i entering the stack and the enthalpy change of reaction of Eq. (3), respectively; T_{in} is the inlet temperature of the SOFC, and T_{ref} is the reference temperature. Table 1 presents some key design parameters of the SOFC studied in this work (Sedghisigarchi, 2004; Murshed *et al.*, 2007).

Table 1 Design parameters of the SOFC

Item	Value
Cell area (cm^2)	100
Electrode thickness (mm)	0.25
Interconnector thickness (mm)	1.5
Electrode density (g/cm^3)	6.6
Interconnector density (g/cm^3)	6.11
Fuel channel height (mm)	1
Air channel height (mm)	1

3 GA-LSSVR for nonlinear system modeling

3.1 LSSVR

The aim of this study is to find a regression function $f(x)$ based on the given training data set, which can be used to precisely predict the output property. A training data set is assumed to be $\{(\boldsymbol{x}_i, \boldsymbol{y}_i), i=1, 2, \ldots, N\}\in\mathbb{R}^n\times\mathbb{R}$, where $\boldsymbol{x}_i$ is the input vector, and $\boldsymbol{y}_i$ is the output vector. The regression function is usually formulated as

$$y(\boldsymbol{x}_i)=f(\boldsymbol{x}_i)=\boldsymbol{w}^{\mathrm{T}}\boldsymbol{\phi}(\boldsymbol{x}_i)+b, \tag{29}$$

where $\boldsymbol{\phi}(\boldsymbol{x}_i)$ is a nonlinear mapping function, which maps the original input data to a high dimensional space, $\boldsymbol{w}$ is the weight vector in the feature space, and b is the bias term.

The optimization problem for the LSSVR model is formulated as

$$\min_{\boldsymbol{w},b,\boldsymbol{e}}J(\boldsymbol{w},\boldsymbol{e})=\frac{1}{2}\boldsymbol{w}^{\mathrm{T}}\boldsymbol{w}+\frac{1}{2}C\sum_{i=1}^{N}e_i^2,\quad C>0, \tag{30}$$

$$\text{s.t.}\quad \boldsymbol{y}_i = \boldsymbol{w}^{\mathrm{T}}\boldsymbol{\phi}(\boldsymbol{x}_i) + b + e_i, \quad i = 1, 2, ..., N, \tag{31}$$

where C (a positive constant) is called the regularization parameter which is used for avoiding over-fitting, and e_i is the error between the actual and the predicted outputs.

To solve the optimization problem, we construct the Lagrangian as follows:

$$\begin{aligned} L(\boldsymbol{w}, b, \boldsymbol{e}, \boldsymbol{\alpha}) = {} & \frac{1}{2}\boldsymbol{w}^{\mathrm{T}}\boldsymbol{w} + \frac{1}{2}C\sum_{i=1}^{N} e_i^2 \\ & - \sum_{i=1}^{N} \alpha_i \{\boldsymbol{w}^{\mathrm{T}}\boldsymbol{\phi}(\boldsymbol{x}_i) + b + e_i - \boldsymbol{y}_i\}, \end{aligned} \tag{32}$$

where α_i (i=1, 2, …, N) is called the Lagrange multiplier. The conditions for optimality can be obtained by solving the following partial differential equations:

$$\begin{aligned} \frac{\partial L}{\partial \boldsymbol{w}} = 0 \rightarrow \quad & \boldsymbol{w} = \sum_{i=1}^{N} \alpha_i \boldsymbol{\phi}(\boldsymbol{x}_i), \\ \frac{\partial L}{\partial b} = 0 \rightarrow \quad & \sum_{i=1}^{N} \alpha_i = 0, \\ \frac{\partial L}{\partial e_i} = 0 \rightarrow \quad & \alpha_i = C e_i, \quad i = 1, 2, \cdots, N, \\ \frac{\partial L}{\partial \alpha_i} = 0 \rightarrow \quad & y_i = \boldsymbol{w}^{\mathrm{T}}\boldsymbol{\phi}(\boldsymbol{x}_i) + b + e_i, \quad i = 1, 2, \cdots, N. \end{aligned} \tag{33}$$

By some simple algebraic manipulations, after eliminating $\boldsymbol{w}$ and $\boldsymbol{e}$, the matrix equation only relative to $\boldsymbol{\alpha}$ and b is obtained as

$$\begin{bmatrix} \boldsymbol{0} & \boldsymbol{1}^{\mathrm{T}} \\ \boldsymbol{1} & \boldsymbol{\Omega} + C^{-1}\boldsymbol{I} \end{bmatrix} \begin{bmatrix} b \\ \boldsymbol{\alpha} \end{bmatrix} = \begin{bmatrix} 0 \\ \boldsymbol{y} \end{bmatrix}, \tag{34}$$

where

$\boldsymbol{1} = [1, 1, \cdots, 1]^{\mathrm{T}}$, $\boldsymbol{y} = [y_1, y_2, \cdots, y_N]^{\mathrm{T}}$, $\boldsymbol{\alpha} = [\alpha_1, \alpha_2, \cdots, \alpha_N]^{\mathrm{T}}$, and

$$\Omega_{i,j} = \boldsymbol{\phi}(\boldsymbol{x}_i)^{\mathrm{T}}\boldsymbol{\phi}(\boldsymbol{x}_j) = K(\boldsymbol{x}_i, \boldsymbol{x}_j), \quad i, j = 1, 2, \cdots, N.$$

Therefore, the LSSVR model can be obtained by

$$\boldsymbol{y}(\boldsymbol{x}) = \sum_{i=1}^{N} \alpha_i K(\boldsymbol{x}, \boldsymbol{x}_i) + b. \tag{35}$$

$K(\boldsymbol{x}, \boldsymbol{x}_i)$ is the kernel function. In this study, the radial basis function (RBF) kernel, i.e., $K(\boldsymbol{x}, \boldsymbol{x}_i) = \exp(-\|\boldsymbol{x}-\boldsymbol{x}_i\|2/(2\sigma^2))$, where σ is the kernel function parameter, is selected because the RBF kernel function has been widely used in a lot of nonlinear regression problems. Furthermore, there exist few parameters to be determined.

To achieve high regression performance, the hyper-parameters should be accurately chosen and this is a key issue in LSSVR modeling. To establish an efficient LSSVR model for the SOFC, two essential hyper-parameters, i.e., the regularization parameter C and the kernel function parameter σ, have to be carefully chosen in advance. The parameter C ascertains the compromise between the training error and the model complexity. The kernel parameter σ defines the variance of the nonlinear mapping function. A too small σ will lead to over-fitting, while a too big σ will result in lower modeling accuracy but higher generalization performance.

Generally, the CV techniques are widely adopted to choose the values of the LSSVR's hyper-parameters, but they are computationally expensive. GA is a kind of evolutionary algorithm. It has been successfully used to solve a great number of optimization problems in different fields. To build a more accurate LSSVR model for the SOFC, GA is used simultaneously to optimize the LSSVR's hyper-parameters for increasing the modeling accuracy and generalization ability.

3.2 Optimization of the LSSVR's parameters based on GA

The hyper-parameters optimization process of the GA-LSSVR model is depicted in Fig. 2. GA is adopted to seek the optimal combination of the LSSVR's parameters so as to obtain a smaller root mean square error (RMSE) during the LSSVR modeling. The detailed description of the optimization steps for the LSSVR's parameters is as follows (Hsu *et al.*, 2006; Yan, 2009; Yang *et al.*, 2010; Yang and Shieh, 2010; Qu and Zuo, 2012):

Step 1. Both LSSVR's hyper-parameters, C and σ^2, are directly coded in binary to randomly construct the chromosome. Here, each chromosome consists of 20 bit binary numbers.

Step 2. To obtain the optimal LSSVR's parameters, a fitness function must be specified in advance

for assessing the performance of each chromosome. In this study, the RMSE is selected as the fitness function for evaluating the modeling accuracy of the GA-LSSVR model. The fitness function is defined as

$$\mathrm{RMSE}=\sqrt{\frac{1}{N}\sum_{i=1}^{N}(y_i-\hat{y}_i)^2}, \tag{36}$$

where y_i and $\hat{y}_i$ are the actual and the predicted values, respectively.

Step 3. The roulette wheel selection (fitness-proportional selection) strategy is adopted to select the chromosomes with the highest fitness values to reproduce.

Step 4. After duplicating, the single-point crossover is applied to generate a new population by exchanging the parent chromosomes information at the assigned positions.

Step 5. The mutation operation with a smaller mutation operator, which is beneficial to the diversity of the population, is carried out after the crossover operation. The mutation probability is usually chosen within the limit of [0.001, 0.1].

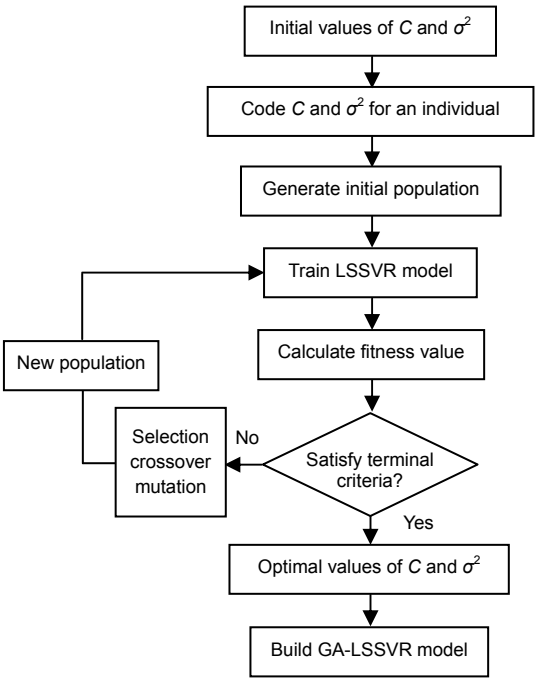

Fig. 2 Process of optimizing the LSSVR's parameters based on GA

Step 6. The maximum evolutional generation is selected as the termination criterion in this study. If the stopping condition is not reached, we must repeat steps 2 to 5 until the termination criterion is met.

Step 7. When the termination condition is satisfied, the optimal combination of the hyper-parameters, C and σ^2, is used to construct the desired SOFC dynamic model.

4 Modeling the SOFC based on GA-LSSVR

4.1 Identification structure of the SOFC stack

A nonlinear autoregressive model with exogenous inputs (NARX) is usually used to describe a wide class of discrete-time nonlinear systems. Therefore, the thermal and electrochemical dynamic characteristics of the SOFC can be represented by the following NARX model:

$$\begin{aligned}\boldsymbol{y}(k+1)=f[&\boldsymbol{y}(k),\boldsymbol{y}(k-1),...,\ \boldsymbol{y}(k-n_y),\\ &\boldsymbol{x}(k),\boldsymbol{x}(k-1),...,\ \boldsymbol{x}(k-n_x)],\end{aligned} \tag{37}$$

where $\boldsymbol{y}(k)$ and $\boldsymbol{x}(k)$ are the output and input vectors at the time step k of the SOFC, respectively, n_y is the output lag, n_x is the input lag, and $f(\cdot)$ is a unknown nonlinear function needed to be identified. To analyze the load tracking performance and the temperature dynamic characteristics of the SOFC simultaneously, we choose $\boldsymbol{x}(k)=[q_{\mathrm{H_2}}^{\mathrm{in}}(k),q_{\mathrm{O_2}}^{\mathrm{in}}(k),I(k)]$ (i.e., the gas molar flow rates of the inlet hydrogen and inlet oxygen, and the stack current) as the input vector and $\boldsymbol{y}(k)=[V_{\mathrm{s}}(k),T_{\mathrm{s}}(k)]$ (i.e., the stack voltage and the operating temperature) as the output vector.

Providing that

$$\begin{aligned}\tilde{\boldsymbol{x}}(k)=[&\boldsymbol{y}(k),\boldsymbol{y}(k-1),\cdots,\boldsymbol{y}(k-n_y),\boldsymbol{x}(k),\\ &\boldsymbol{x}(k-1),\cdots,\boldsymbol{x}(k-n_x)],\quad k=1,2,\cdots,N,\end{aligned} \tag{38}$$

we have

$$\boldsymbol{y}(k+1)=f(\tilde{\boldsymbol{x}}(k)). \tag{39}$$

Based on the collected training data set $(\tilde{\boldsymbol{x}}(k),\ \boldsymbol{y}(k+1))$, the following LSSVR model can be constructed using the LSSVR theory:

$$\hat{\boldsymbol{y}}(k+1)=\sum_{i=1}^{N}\alpha_i K(\tilde{\boldsymbol{x}}(k),\boldsymbol{x}_i)+b. \tag{40}$$

4.2 Preparation of the simulation data

In this study, the SOFC stack can be regarded as a system with three inputs and two outputs. The nominal operating parameters of the SOFC are given in Table 2 (Padullés *et al.*, 2000; Murshed *et al.*, 2007). Using the physical dynamic model, the modeling data for the GA-LSSVR model can be gathered. When the load step changes from 500 A to 600 A at t=200 s and from 600 A to 450 A at t=600 s, a group of input/output data $([q_{\mathrm{H}_2}^{\mathrm{in}}(i), q_{\mathrm{O}_2}^{\mathrm{in}}(i), I(i), V_{\mathrm{s}}(i), T_{\mathrm{s}}(i)]$, i=1, 2, …, 1000) is collected by means of simulation when the sampling time is set as 1 s. The database consisting of 1000 cases with five dimensions is also divided into two sets. Here, the data $[q_{\mathrm{H}_2}^{\mathrm{in}}(1)$, $q_{\mathrm{O}_2}^{\mathrm{in}}(1)$, $I(1)$, $V_{\mathrm{s}}(1)$, $T_s(1)$; $q_{\mathrm{H}_2}^{\mathrm{in}}(2)$, $q_{\mathrm{O}_2}^{\mathrm{in}}(2)$, $I(2)$, $V_{\mathrm{s}}(2)$, $T_{\mathrm{s}}(2)$; …; $q_{\mathrm{H}_2}^{\mathrm{in}}(800)$, $q_{\mathrm{O}_2}^{\mathrm{in}}(800)$, $I(800)$, $V_{\mathrm{s}}(800)$, $T_{\mathrm{s}}(800)]$ is selected as the training set to identify the GA-LSSVR model of the SOFC, and the data [$V_{\mathrm{s}}(2)$, $T_{\mathrm{s}}(2)$; $V_{\mathrm{s}}(3)$, $T_{\mathrm{s}}(3)$; …; $V_{\mathrm{s}}(1000)$, $T_{\mathrm{s}}(1000)$] is chosen as the testing set to validate the established GA-LSSVR model.

Table 2 Nominal operating parameters of the SOFC

Item	Value
N_0	384
T_{in} (K)	973
I_{rate} (A)	500
E_0 (V)	1.18
K_{H_2} (mol/(s·atm))	0.843
K_{O_2} (mol/(s·atm))	2.52
$K_{\mathrm{H_2O}}$ (mol/(s·atm))	0.281
τ_{H_2} (s)	26.1
τ_{O_2} (s)	2.91
$\tau_{\mathrm{H_2O}}$ (s)	78.3
r (Ω)	0.126
$q_{\mathrm{H}_2,\mathrm{rate}}^{\mathrm{in}}$ (mol/s)	5
$q_{\mathrm{O}_2,\mathrm{rate}}^{\mathrm{in}}$ (mol/s)	10
$\Delta\hat{H}_{\mathrm{r}}^{0}$ (J/mol)	-0.2418×10^6
$\bar{C}_{\mathrm{ps}}$ (J/(g·K))	0.4

To eliminate the dimension differences, all the training and testing data should be normalized in the range of [0, 1] by

$$x_{\mathrm{norm}}=\frac{x_i-x_{\min}}{x_{\max}-x_{\min}}. \tag{41}$$

4.3 Selection of the optimal LSSVR parameters

To build an efficient LSSVR model for the SOFC, two parameters of the LSSVR, C and σ^2, must be carefully determined. In contrast with the CV methods, GA is adopted to seek the optimal combination of the LSSVR's parameters in this study.

During the LSSVR modeling, the extents of the parameters C and σ^2 are distributed in (0, 100] and [0, 1000], respectively. The original population size of GA is P=20, the maximum iterations is 200, each chromosome consists of 20 bit binary numbers, and the probabilities of the crossover and the mutation are selected as p_{c}=0.4 and p_{m}=0.01, respectively. Then, the identification model of the SOFC can be constructed using the optimal LSSVR's parameters for predicting.

4.4 Identification results of the GA-LSSVR model

By minimizing the RMSE, a GA-LSSVR model of the SOFC is established based on the training data using the optimal parameters obtained in Section 4.3. To further assess the predicting performance of the GA-LSSVR model, the voltage and the temperature dynamic characteristics of the SOFC will be simulated under different conditions. For comparison, the standard LSSVR whose parameters are determined by a simulated annealing algorithm (SAA-LSSVR) is used to model the same plant. During the modeling, the initial temperature of the SAA is set to 280°, the length of the MapkoB chain is 300, and the step lengths for parameters C and σ^2 are both selected as 0.2. In addition, the corresponding results of the LSSVR with a 5-fold cross-validation (5FCV-LSSVR) model are also presented.

When the load changes from 500 A to 600 A at t=200 s and from 600 A to 450 A at t=600 s, it executes the simulations for the output voltage and the temperature dynamics of the SOFC. Fig. 3a depicts the output voltage of the physical model and the predicting results of the GA-LSSVR model. Furthermore, the simulation results for the output voltage of the

SAA-LSSVR and the 5FCV-LSSVR models under the same load conditions are also shown in Figs. 3b and 3c, respectively. Fig. 4a gives the temperature comparison between the GA-LSSVR and the physical models in this load situation. At the same time, the predicted temperature of the SAA-LSSVR model and the 5FCV-LSSVR model are described in Figs. 4b and 4c, respectively.

Figs. 3a and 4a show that the prediction results of the established GA-LSSVR model almost agree with those of the physical model, indicating that the GA-LSSVR model is valid for dynamic performance prediction of the SOFC.

By comparing the simulation results of the output voltage among Figs. 3a–3c, and the prediction results of the temperature among Figs. 4a–4c, one

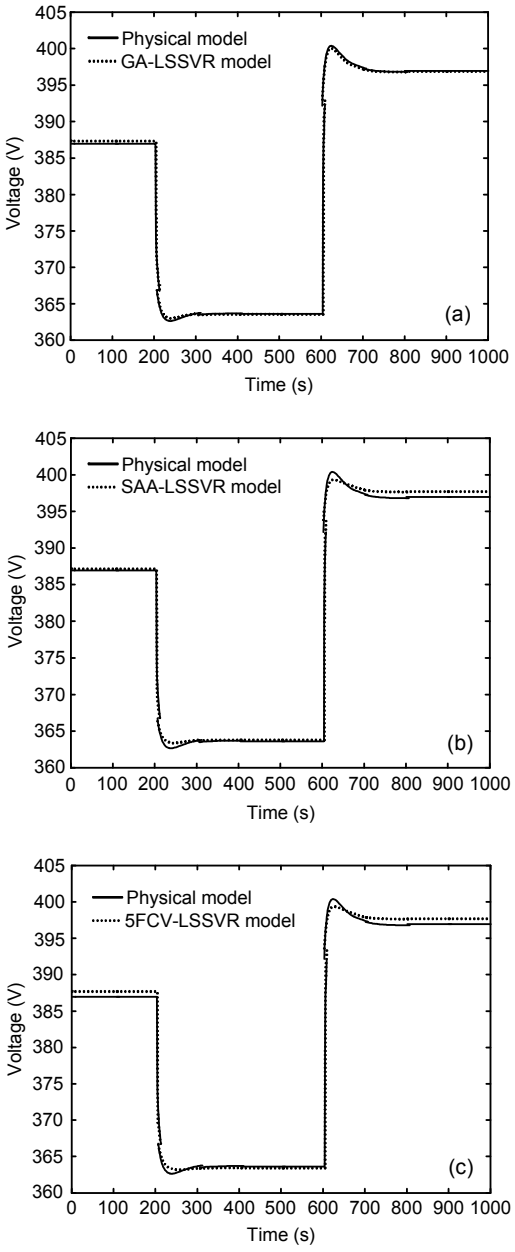

Fig. 3 Output voltage responses of the physical model and the models of GA-LSSVR (a), SAA-LSSVR (b), and 5FCV-LSSVR (c)

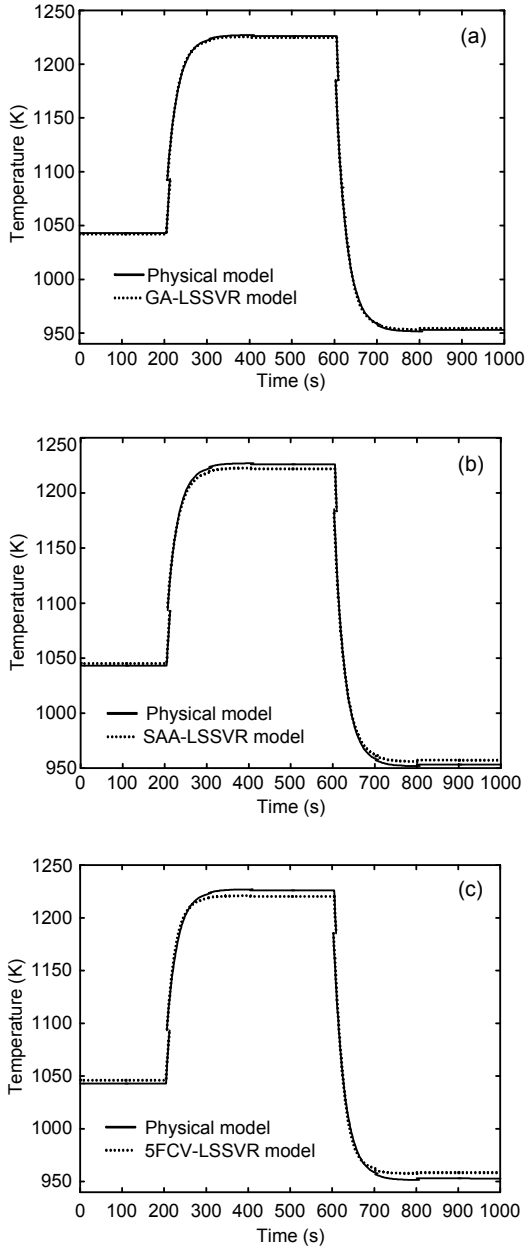

Fig. 4 Temperature responses of the physical model and the models of GA-LSSVR (a), SAA-LSSVR (b), and 5FCV-LSSVR (c)

will notice that the prediction performance of the GA-LSSVR model for the SOFC has been greatly improved.

To further evaluate the modeling accuracy of the GA-LSSVR model, the mean relative error (MRE) and the RMSE of the GA-LSSVR, the SAA-LSSVR, and the 5FCV-LSSVR models for the output voltage and the temperature are given in Tables 3 and 4, respectively. Moreover, in our study, the prediction time of the GA-LSSVR, the SAA-LSSVR, and the 5FCV-LSSVR models are also recorded in Table 5. The results indicate that compared with the 5FCV-LSSVR technique, the GA-LSSVR can simultaneously predict the output voltage and the temperature dynamics of the SOFC with a higher accuracy and a faster convergence rate. In addition, in comparison with the SAA-LSSVR method, the GA-LSSVR model needs a little more time to predict the output voltage characteristics of the SOFC; however, the GA-LSSVR has a higher precision accuracy in appropriating both the output voltage and the temperature.

Table 3 MRE of the GA-LSSVR, the SAA-LSSVR, and the 5FCV-LSSVR models

Model type	MRE	
	Stack voltage (V)	Operating temperature (K)
GA-LSSVR	0.0935	0.1039
SAA-LSSVR	0.1174	0.3149
5FCV-LSSVR	0.1432	0.4150

Table 4 RMSE from the GA-LSSVR, the SAA-LSSVR, and the 5FCV-LSSVR models

Model type	RMSE	
	Stack voltage (V)	Operating temperature (K)
GA-LSSVR	0.7823	1.8641
SAA-LSSVR	0.8952	3.6504
5FCV-LSSVR	10.4085	4.7680

Table 5 Prediction time of the GA-LSSVR, the SAA-LSSVR, and the 5FCV-LSSVR models

Model type	Prediction time (s)	
	Stack voltage	Operating temperature
GA-LSSVR	416.6730	133.3348
SAA-LSSVR	370.8479	186.0621
5FCV-LSSVR	563.6533	518.5528

5 Conclusions

To investigate the dynamic behaviors of the SOFC and facilitate the model-based controller design, the LSSVR identification model whose parameters are optimized by GA is proposed to simultaneously describe the electrochemical and thermal characteristics of the SOFC. The performance of the GA-LSSVR model has been tested and compared with the SAA-LSSVR and the 5FCV-LSSVR models. The results indicate that the prediction accuracy of the GA-LSSVR model has been immensely improved; in addition, its convergence rate is much faster. These results verified the applicability of the GA-LSSVR model in modeling the transient behaviors of the SOFC. It provides the foundation for further study of the dynamic characteristics of the SOFC under different conditions considering valid control strategies.

References

Bove, R., Ubertini, S., 2006. Modeling solid oxide fuel cell operation: approaches, techniques and results. *Journal of Power Sources*, **159**(1):543-559. [doi:10.1016/j.jpowsour.2005.11.045]

Cao, H.L., Deng, Z.H., Li, X., *et al*., 2010. Dynamic modeling of electrical characteristics of solid oxide fuel cells using fractional derivatives. *International Journal of Hydrogen Energy*, **35**(4):1749-1758. [doi:10.1016/j.ijhydene.2009.11.103]

Chakraborty, U.K., 2011. An error in solid oxide fuel cell stack modeling. *Energy*, **36**(2):801-802. [doi:10.1016/j.energy.2010.12.038]

Entchev, E., Yang, L.B., 2007. Application of adaptive neuro-fuzzy inference system techniques and artificial neural networks to predict solid oxide fuel cell performance in residential microgeneration installation. *Journal of Power Sources*, **170**(1):122-129. [doi:10.1016/j.jpowsour.2007.04.015]

Ge, Z.Q., Song, Z.H., 2008. Online monitoring of nonlinear multiple mode processes based on adaptive local model approach. *Control Engineering Practice*, **16**(12):1427-1437. [doi:10.1016/j.conengprac.2008.04.004]

Hajimolana, S.A., Tonekabonimoghadam, S.M., Hussain, M.A., *et al.*, 2013. Thermal stress management of a solid oxide fuel cell using neural network predictive control. *Energy*, **62**:320-329. [doi:10.1016/j.energy.2013.08.031]

Hsu, C.C., Wu, C.H., Chen, S.C., *et al*., 2006. Dynamically optimizing parameters in support vector regression: an application of electricity load forecasting. Proceedings of the 39th Annual Hawaii International Conference on System Sciences, Kauai, USA, p.30c. [doi:10.1109/HICSS.2006.132]

Huo, H.B., Zhong, Z.D., Zhu, X.J., *et al*., 2008. Nonlinear dynamic modeling for a SOFC stack by using a Hammerstein model. *Journal of Power Sources*, **175**(1):441-446. [doi:10.1016/j.jpowsour.2007.09.059]

Jiang, J.H., Li, X., Deng, Z.H., *et al*., 2013. Control-oriented dynamic model optimization of steam reformer with an improved optimization algorithm. *International Journal of Hydrogen Energy*, **38**(26):11288-11302. [doi:10.1016/j.ijhydene.2013.06.103]

Jurado, F., 2004. Modeling SOFC plants on the distribution system using identification algorithms. *Journal of Power Sources*, **129**(2):205-215. [doi:10.1016/j.jpowsour.2003.11.035]

Kazempoor, P., Ommi, F., Dorer, V., 2011. Response of a planar solid oxide fuel cell to step load and inlet flow temperature changes. *Journal of Power Sources*, **196**(21):8948-8954. [doi:10.1016/j.jpowsour.2011.01.047]

Kim, Y., Son, M., Lee, I.B., 2011. Numerical study of a planar solid oxide fuel cell during heat-up and start-up operation. *Industrial and Engineering Chemistry Research*, **50**(3):1360-1368. [doi:10.1021/ie100783g]

Li, J., Kang, Y.W., Cao, G.Y., *et al*., 2008. Numerical simulation of a direct internal reforming solid oxide fuel cell using computational fluid dynamics method. *Journal of Zhejiang University-SCIENCE A*, **9**(7):961-969. [doi:10.1631/jzus.A0720054]

Lu, N., Li, Q., Sun, X., *et al*., 2006. The modeling of a standalone solid-oxide fuel cell auxiliary power unit. *Journal of Power Sources*, **161**(2):938-948. [doi:10.1016/j.jpowsour.2006.05.009]

Mao, W.T., Yan, G.R., Dong, L.L., *et al*., 2011. Model selection for least squares support vector regressions based on small-world strategy. *Expert Systems with Applications*, **38**(4):3227-3237. [doi:10.1016/j.eswa.2010.08.109]

Menon, V., Janardhanan, V.M., Tischer, S., *et al*., 2012. A novel approach to model the transient behavior of solid-oxide fuel cell stacks. *Journal of Power Sources*, **214**:227-238. [doi:10.1016/j.jpowsour.2012.03.114]

Murshed, A.M., Huang, B., Nandakumar, K., 2007. Control relevant modeling of planer solid oxide fuel cell system. *Journal of Power Sources*, **163**(2):830-845. [doi:10.1016/j.jpowsour.2006.09.080]

Padullés, J., Ault, G.W., McDonald, J.R., 2000. An integrated SOFC plant dynamic model for power systems simulation. *Journal of Power Sources*, **86**(1-2):495-500. [doi:10.1016/S0378-7753(99)00430-9]

Qu, J., Zuo, M.J., 2012. An LSSVR-based algorithm for online system condition prognostics. *Expert Systems with Applications*, **39**(5):6089-6102. [doi:10.1016/j.eswa.2011.12.002]

Salogni, A., Colonna, P., 2010. Modeling of solid oxide fuel cells for dynamic simulations of integrated systems. *Applied Thermal Engineering*, **30**(5):464-477. [doi:10.1016/j.applthermaleng.2009.10.007]

Sedghisigarchi, K., 2004. Solid Oxide Fuel Cell as a Distributed Generator: Dynamic Modeling, Stability Analysis and Control. PhD Thesis, West Virginia University, Morgantown, USA.

So-ryeok, O., Jing, S., Herb, D., *et al*., 2013. Dynamic characteristics and fast load following of 5-kW class tubular solid oxide fuel cell/micro-gas turbine hybrid systems. *International Journal of Energy Research*, **37**(10):1242-1255. [doi:10.1002/er.3031]

Suykens, J.A.K., van Gestel, T., de Brabanter, J., *et al*., 2002. Least Squares Support Vector Machines. World Scientific, Singapore, p.98-114.

Wang, H., Li, E., Li, G.Y., 2011. Probability-based least square support vector regression metamodeling technique for crashworthiness optimization problems. *Computational Mechanics*, **47**(3):251-263. [doi:10.1007/s00466-010-0532-y]

Wang, L.J., Zhang, H.S., Weng, S.L., 2008. Modeling and simulation of solid oxide fuel cell based on the volume-resistance characteristic modeling technique. *Journal of Power Sources*, **177**(2):579-589. [doi:10.1016/j.jpowsour.2007.10.051]

Wu, X.J., Huang, Q., Zhu, X.J., 2011. Thermal modeling of a solid oxide fuel cell and micro gas turbine hybrid power system based on modified LS-SVM. *International Journal of Hydrogen Energy*, **36**(1):885-892. [doi:10.1016/j.ijhydene.2010.08.022]

Xu, G.M., Huang, S.G., 2011. Runway incursion event forecast model based on LS-SVR with multi-kernel. *Journal of Computers*, **6**(7):1346-1352. [doi:10.4304/jcp.6.7.1346-1352]

Yan, G., 2009. Forecasting of freight volume based on support vector regression optimized by genetic algorithm. The 2nd IEEE International Conference on Computer Science and Information Technology, Beijing, China, p.550-553. [doi:10.1109/ICCSIT.2009.5234798]

Yang, C.C., Shieh, M.D., 2010. A support vector regression based prediction model of affective responses for product form design. *Computers and Industrial Engineering*, **59**(4):682-689. [doi:10.1016/j.cie.2010.07.019]

Yang, J., Li, X., Mou, H.G., *et al*., 2009. Control-oriented thermal management of solid oxide fuel cells based on a modified Takagi-Sugeno fuzzy model. *Journal of Power Sources*, **188**(2):475-482. [doi:10.1016/j.jpowsour.2008.12.012]

Yang, Z., Gu, X.S., Liang, X.Y., *et al*., 2010. Genetic algorithm-least squares support vector regression based predicting and optimizing model on carbon fiber composite integrated conductivity. *Materials and Design*, **31**(3):1042-1049. [doi:10.1016/j.matdes.2009.09.057]

Zhang, T.J., Feng, G., 2009. Rapid load following of an SOFC power system via stable fuzzy predictive tracking controller. *IEEE Transactions on Fuzzy Systems*, **17**(2):357-371. [doi:10.1109/TFUZZ.2008.2011135]

中文概要：

本文题目： 基于遗传算法优化最小二乘支持向量回归机的平板型固体氧化物燃料电池的控制相关动态辨识建模

Control-oriented dynamic identification modeling of a planar SOFC stack based on genetic algorithm-least squares support vector regression

研究目的： 为了同时预测固体氧化物燃料电池（SOFC）的电压、温度动态特性和设计控制器，建立 SOFC 的控制相关动态辨识模型。

创新要点： 为了建立 SOFC 更精确的最小二乘支持向量回归机（LSSVR）动态模型，采用遗传算法（GA）优化 LSSVR 的参数。所建 GA-LSSVR 模型可同时预测 SOFC 的电压和温度动态特性。

研究方法： 1. 分析 SOFC 的电化学和能量平衡子模型。2. 利用所选择的最优 LSSVR 参数，建立了 SOFC 的 GA-LSSVR 动态辨识模型。通过仿真分析和比较，验证了所建模型的有效性（图 3 和 4）。3. 利用所建模型的预测结果，与模拟退火算法优化最小二乘支持向量回归机（SAA-LSSVR）和 5 折交叉验证最小二乘支持向量回归机（5FCV-LSSVR）模型的预测结果进行了比较，表明所建立的 GA-LSSVR 模型具有较高的预测精度（表 3 和 4）。

重要结论： 通过比较 SAA-LSSVR 和 5FCV-LSSVR 模型的预测结果，发现所建 GA-LSSVR 模型具有较好的预测性能和精度。基于所建立的 GA-LSSVR 模型可进行有效的多变量控制器设计。

关键词组： 固体氧化物燃料电池（SOFC）；控制相关；动态建模；最小二乘支持向量回归机